

1 Article

2 Gesture-based control of a robot arm with 3 neuromorphic haptic feedback

4 F. Sorgini^{1†}, G. Airò Farulla^{2,3†}, N. Lukic^{4†}, I. Danilov^{4†}, B. Bojovic⁴, M. Milivojevic⁴, T. B.
5 Pulikottil⁵, L. Roveda⁵, P. Prinetto^{2,3}, T. Tolio^{5,6}, M.C. Carrozza^{1,7}, P.B. Petrovic^{4,8*†} and C.M.
6 Oddo^{1*†}

7 ¹ The BioRobotics Institute, Scuola Superiore Sant'Anna, Pisa, Italy

8 ² Department of Control and Computer Engineering, Politecnico di Torino

9 ³ CINI AsTech National Lab, Turin, Italy

10 ⁴ Production Engineering Department, Faculty of Mechanical Engineering, University of Belgrade, Belgrade,
11 Serbia

12 ⁵ Istituto di Sistemi e Tecnologie Industriali per il Manifatturiero Avanzato (STIIMA) – CNR, Milano, Italy

13 ⁶ Dipartimento di Meccanica, Politecnico di Milano, Milano, Italy

14 ⁷ IRCCS Fondazione Don Carlo Gnocchi, Milano, Italy

15 ⁸ Academy of Engineering Sciences of Serbia-AISS, Belgrade, Serbia

16

17 * Correspondence: calogero.oddo@santannapisa.it, pbpetrovic@mas.bg.ac.rs

18 † These authors share first authorship based on equal contribution

19 ‡ These authors share senior authorship based on equal contribution

20

21 **Abstract:** Research on bidirectional human-machine interfaces will enable the smooth interaction
22 with robotic platforms in contexts ranging from industry to tele-medicine and rescue. This paper
23 introduces a bidirectional communication system to achieve multisensory telepresence during the
24 gestural control of an industrial robotic arm. We complement the gesture-based control by means
25 of a tactile-feedback strategy grounding on a spiking artificial neuron model. Force and motion from
26 the robot are converted in neuromorphic haptic stimuli delivered on the user's hand through a
27 vibro-tactile glove. Untrained personnel participated in an experimental task benchmarking a pick-
28 and-place operation. The robot end-effector was used to sequentially press six buttons, illuminated
29 according to a random sequence, and comparing the tasks executed without and with tactile
30 feedback. The results demonstrated the reliability of the hand tracking strategy developed for
31 controlling the robotic arm, and the effectiveness of a neuronal spiking model for encoding hand
32 displacement and exerted forces in order to promote a fluid embodiment of the haptic interface and
33 control strategy. The main contribution of this paper is in presenting a robotic arm under gesture-
34 based remote control with multisensory telepresence, demonstrating for the first time that a spiking
35 haptic interface can be used to effectively deliver on the skin surface a sequence of stimuli emulating
36 the neural code of the mechanoreceptors beneath.

37 **Keywords:** telepresence; neuromorphic vibrotactile feedback; human-robot interaction; hand
38 tracking; gesture-based teleoperation.

39

40 1. Introduction

41 In the last decades, research about the development of human-robot interfaces for the remote
42 control of robotic systems has gained momentum in a variety of contexts like manufacturing [1,2],
43 search and rescue [3], dangerous operations [4,5], and robotic surgery [6,7]. Especially in
44 manufacturing environments, human-robot interfaces are introduced for collaboration and co-
45 working purposes (CoBots), demanding various kind of physical and cognitive interactions between
46 humans and robots, i.e. biological and engineered systems. The importance of teleoperation resides

47 in the presence of a human individual in the control loop, especially in critical situations where
48 human supervision can avoid faults or dangers [8,9]. Until recently, the main instruments to interact
49 with robotic platforms were relatively constrained gamepad, joystick and keyboard interface devices.
50 Progress in the field of Human Robot Interaction (HRI) is introducing innovative devices which
51 empower users to interact with computer systems in increasingly natural and intuitive ways. Systems
52 adopting these technologies show improved efficiency, speed, power, and realism. Ideally, new
53 interfaces should be accessible without requiring long periods of training and adaptation [10].

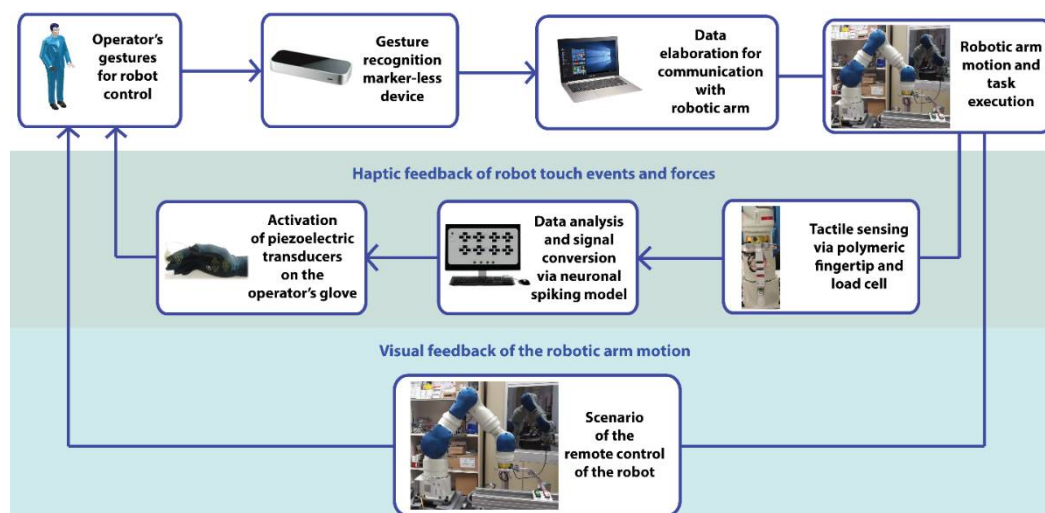
54 Vision-based Pose Estimation (VPE) and Hand Tracking techniques have played a leading role
55 in the field of HRI, and already demonstrated their applicability to remote control of robotic actuators
56 [11] in a variety of domains, including tele-rehabilitation and telemedicine [12]. Furthermore, VPE
57 interfaces are typically intuitive enough to be used even by untrained personnel [10]. Vision systems
58 can be used to control disparate dynamic systems like for example vehicles, aircrafts and submarines,
59 and are classified depending on the number of cameras required in their set-ups. Specifically, single
60 camera-based systems are generally cheaper and easier to build than multi-camera ones [13,14]. An
61 example of camera-based set-up involves the Leap Motion controller [15], a binocular camera system
62 operating in the IR domain (gray-scale system), based on its own IR source. The recent introduction
63 of this hand tracking device has opened new opportunities for hand tracking and hand gesture
64 recognition: it has proven to be precise and reliable both in static and dynamic conditions for hand
65 tracking [16,17]. Differently from RGB-D cameras, the Leap Motion controller explicitly targets the
66 task of tracking the hand pose. Even though its interaction zone is rather limited, the extracted data
67 are very accurate and it is not necessary to perform image processing tasks to extract the relevant
68 points. Authors in [18] report that, although they were not able to achieve the theoretical accuracy of
69 0.01mm under real conditions, still the controller provided high precision standards, not achievable
70 with RGB-cameras in the same price range (with an overall accuracy of 0.7 mm) [19].

71 The delivery of tactile feedback in telepresence operations is fundamental to augment users'
72 immersivity; examples can be found in minimally invasive surgery [6] and in industrial operations
73 [3,20-22] and manufacturing [23]. In this context, where robots are mainly involved in object
74 manipulation tasks, tactile feedback can help in performing high-precision activities keeping the
75 human operator in the loop. Tactile feedback technologies to deliver real-time information are
76 common in literature though there is still a lack of their in-field application. The sense of touch is one
77 of the first ways we use to interact with the surrounding world, especially through our hands which
78 represent the most somatosensitive part of the body [24,25]. In particular, human hands' skin is able
79 to perceive a relatively wide range of frequencies when stimulated with a vibrotactile stimulus, with
80 a maximum frequency centered at about 300 Hertz for Pacinian receptors [26-29]. The maximum
81 spatial sensitivity is achieved on the index phalanx, where the location of a presented vibrotactile
82 stimulation is precisely encoded [30].

83 The importance of tactile sense can be better understood when considering all those individuals
84 who experienced its loss. Without tactile information, actions like using tools, holding objects or
85 motor control tasks can become extremely difficult if not impossible to perform [31]. In all those
86 situations where a fine control of mechanical tools or robotic hands is required, the possibility to
87 deliver information from the environment directly on users' skin via tactile feedback can enhance the
88 performance of executed tasks. The activation of a force feedback real-time channel, coming from the
89 sensing elements on the robot, allows the user to receive the aggregated profiles of exerted forces.
90 Touch feedback allows the user to collect information from the contact points (a force array), and the
91 observed pressure patterns can give information about the surface shape and texture, or about
92 objects' stiffness [32].

93 In this work, we are focused on distant human-robot bidirectional physical interaction. We
94 propose a novel paradigm for controlling a robot interface via vision-based marker-less technology
95 for hand tracking, involving vibrotactile feedback on the user hand triggered by the output of a
96 neuromorphic artificial neuron spiking model in case of robot constrained motion (a physical contact
97 of robot arm and its environment). We implement a telerobotic system in which user hand
98 movements are detected by a hand tracking device (the Leap Motion controller) and serve as

99 commands for a robotic arm performing a generic pick-and-place task. Vibrotactile feedback is
 100 generated via neuronal spiking models and is delivered on the user hand by means of a textile glove
 101 equipped with piezoelectric transducers. The haptic feedback subsystem serves two main purposes:
 102 1) proprioceptive feedback about the user's hand position with respect to the rest position of the
 103 tracking device; 2) exteroceptive feedback about contact events and the amount of the force exerted
 104 by the robot end-effector. To the best of our knowledge, no existing research has already developed
 105 a bidirectional communication channel for the remote control of a robotic arm under multisensory
 106 telepresence, where input for the robot is provided by means of hand tracking technology, and
 107 vibrotactile force feedback is delivered to the users via the implementation of a neuronal spiking
 108 model.



109

110 **Figure 1. Block diagram of the robotic arm with bidirectional gesture control system.** The hand
 111 movements of the operator are recognized by means of marker-less infrared stereo camera and
 112 delivered to the robot as motion commands while the operator is fed back with spiking vibrotactile
 113 stimuli representing the commanded robot velocity and its tactile interaction with the environment.

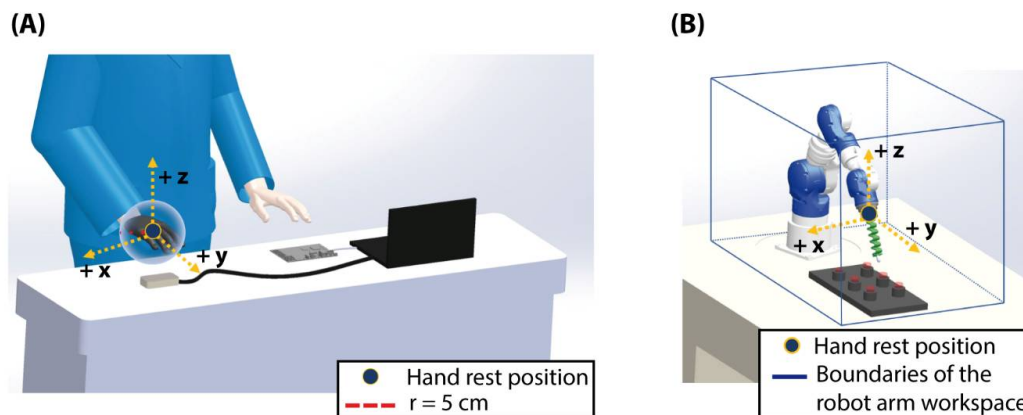
114 2. Materials and Methods

115 In this section, we will firstly present the three main subsystems which constitute our
 116 experimental setup for the remote robot control with tactile telepresence: 1) a hand tracking device
 117 which is used to detect the movements of the hand during the execution of the experimental tasks
 118 and to remotely control a robotic arm; 2) a vibrotactile glove, equipped with two piezoelectric
 119 transducers for the haptic feedback on the operators hand [33]; 3) an anthropomorphic robotic arm,
 120 which mounts a polymeric soft fingertip and a load cell on the end-effector for the button-pressing
 121 task. The experimental protocol is then reported, including description of the participants who took
 122 part in the experiments.

123 2.1 Hand tracking subsystem

124 Within the experimental set-up, the hand tracking device (Leap Motion controller) is connected
 125 to a dedicated Windows laptop (Intel Core™ i7-6500U processor @3.1GHz, 16GB of RAM) via USB
 126 3.0 connection. The interface to this controller has been designed in LabView leveraging on the
 127 LabView MakerHub APIs [15]. The GUI continuously tracks the pose of the right hand of the operator
 128 and uses its global configuration with respect to the origin of the Cartesian space over the controller
 129 to activate the vibrotactile transducer placed on the hand palm with a temporal actuation depending
 130 on the hand displacement from the origin of the 3D space. Communication between the laptop
 131 equipped with the Leap Motion and the PC-based open architecture system for controlling the robot
 132 is managed via an UDP channel.

133 The 3D workspace (Figure 2) for the user to move is defined via the LabView GUI. The rest
 134 position consists of a sphere with 5cm radius, which center (the home “rest” space) can be set via the
 135 same LabView environment. The definition of a rest space allows the robot to stop when the hand
 136 enters inside the 5cm boundaries, as well as the glove to stop the vibration activity of the transducer
 137 associated to “proprioceptive” feedback. At the beginning of each experiment, once the hand is
 138 placed over the device, the hand rest position is acquired by the experimenter as a reference position
 139 in the workspace. Once the hand is moved within the 3D space over the controller, vibration is
 140 delivered to the haptic feedback subsystem according to the current hand displacement with respect
 141 to the rest position. If the hand reaches and crosses the boundaries of the working space, the vibration
 142 stops. The sampling rate to acquire the hand positions is 50Hz.



143

144 **Figure 2. Schematic representation of the robot arm gesture-based control strategy.** (A) The blue
 145 dot represents the hand rest position, a sphere with 5cm radius, corresponding to a stop of the motion
 146 of the robot arm. When the hand moves outside the rest position, the robot arm moves following the
 147 hand displacement, according to the represented coordinates system. In particular, the hand
 148 displacements along the three axes are converted in velocities of the robotic arm along the same
 149 directions. (B) The robot arm moves according to the received commands from the hand-tracking
 150 device, in a space constrained within a 3D cube. If a command from the hand pushes the robot arm
 151 outside the workspace cube, the robot stops.

152 2.2 Neuromorphic haptic feedback subsystem

153 Haptic feedback is delivered by means of a spandex glove equipped with two piezoelectric
 154 transducers, to provide the user with a wearable vibro-tactile display that could be flexible and light,
 155 and to assure a stable positioning of the haptic elements on the user’s hand [32]. The embedded
 156 actuators are piezoelectric disks (7BB-12-9, MuRata) with a diameter of 12mm and a thickness of
 157 220 μ m. They are encapsulated in a polymeric matrix (PDMS, Dow Corning 184 - Silicone Elastomer),
 158 thus resulting in a contact area on the skin of approximately 250mm². Dimensions of the final
 159 elements are 18mm in diameter and 4mm in thickness [33,34].

160 One vibrotactile actuator is integrated in the index finger of the glove, in correspondence of the
 161 index phalanx. The second actuator is instead on the palm.

162 The actuation signal delivered to the piezoelectric element on the index phalanx comes from the
 163 load cell mounted on the robot end effector. The acquired force is converted in spikes according to a
 164 neuronal spiking model. Spikes are then sent to the glove and serve to activate tactile elements. The
 165 spikes firing activity is proportional to the amplitude of the contact force measured by the load cell,
 166 and the presence of the vibration on the index fingertip is representative of the occurrence of a contact
 167 event. The firing activity of the spikes delivered to the piezoelectric element on the palm is instead
 168 related to the hand position along the three spatial axes detected by the hand tracking device. This
 169 signal is controlled by the hand tracking device software. For all transducers, the parameters for the
 170 neuronal spiking model were selected to operate within a range far from saturation, so that the

171 vibrotactile feedback can be proportional to the forces exerted by the robot end effector, and to the
172 displacement of the hand with respect to the rest position defined over the hand tracking device.

173 The activation of both the transducers embedded in the vibrotactile glove is managed by a GUI
174 developed in LabView that receives via UDP communication the forces read by the load cell on the
175 robotic arm end-effector. Hand displacement data recorded from the hand-tracking device are
176 acquired by the computer. The same GUI implements the neuronal spiking algorithm and spikes are
177 delivered to the glove thanks to dedicated electronics. This comprises: an electronic board (sbRIO
178 9636, National Instruments) for the communication between the force signal from the robot and the
179 piezoelectric elements in the glove; a switching circuit with relays, for the selective activation of the
180 two transducers placed on the index and palm, together with their on-off behaviour; a piezoelectric
181 evaluation module (DRV2667, Texas Instruments), working in analog mode, for the activation of the
182 piezoelectric transducers. The analog mode allows the real-time activation of the transducers
183 according to the spikes generated by the model. The actuation parameters for the piezoelectric driver
184 in this mode are a 40.7dB gain, a peak-to-peak voltage amplitude of 200V and a Boost voltage of 105V.
185 The on-off activity of the transducers is instead regulated by the implementation of the Izhikevich
186 neuromorphic model [35,36].

187 The activation of the piezoelectric transducers is triggered by a neuromorphic spiking model
188 which converts the normal force measured by the load cell in spike trains. The Izhikevich neuronal
189 spiking model is discretized via the Euler method, using regular spiking coefficients ($a=0.02s^{-1}V^{-1}$;
190 $b=0.2s^{-1}$; $c=65F$; $d=8mV$). The current provided as an input to the Izhikevich neuron is proportional
191 to the measured interaction force ($I=K|F_z|$). During the experiments, the gain K is set at a value
192 $K_i=10mA/N$ for the feedback on the index finger, and at a value $K_p=0.6mA/N$ for the palm. These
193 values are selected in order to obtain spiking vibrotactile patterns with a rate proportional to the
194 intensity of the applied normal force for the index, and to the amount of target robot velocity
195 commanded by the displacement of the palm with respect to the rest position. The Izhikevich spiking
196 model is implemented via a GUI developed in LabView (2015, National Instruments). The obtained
197 spikes trains are then delivered to the glove by means of the dedicated electronics described in the
198 "Neuromorphic haptic feedback subsystem" Section.

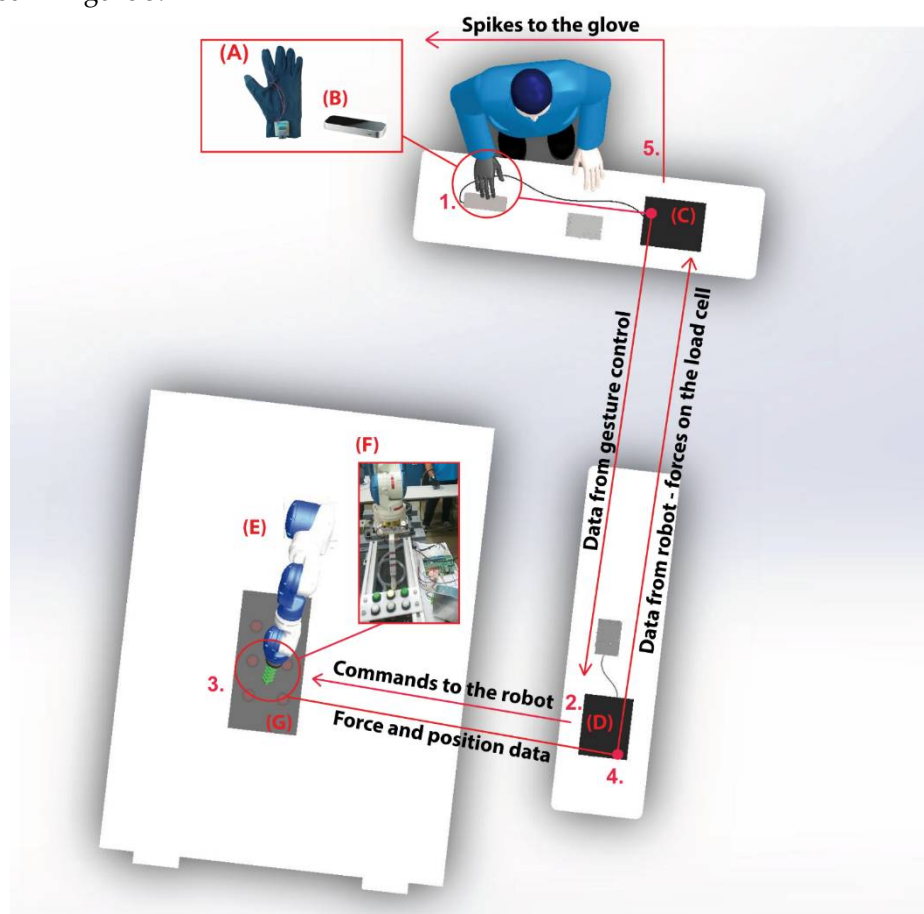
199 *2.3 Anthropomorphic robot arm and test bench*

200 The anthropomorphic arm integrated in the experimental setup is a 7-DoFs robot (SIA10F,
201 Yaskawa Motoman Robotics). It is equipped with a load cell (CZL602, Dongguan South China Sea
202 Electronic Co., Ltd; rated load 3 kg) on its end effector. Force data are acquired and preprocessed by
203 STM 32F415RG ARM Cortex-M4 32-bit RISC core DSP microcontroller, operating at a frequency of
204 168 MHz. The robotic arm is controlled by an open architecture control system, consisting of a high-
205 speed robot controller FS100 (1ms feedback time constant) running VxWorks real-time operating
206 system and associated Yaskawa MotoPuls SDK PC-based high-level controller. This comprehensive
207 API allows to control and monitor the robot functions through Ethernet interface, which is capable
208 to interrupt the execution of the robot controller task in any instant. A passivity-based control law
209 [37,38], well adapted for human-robot co-working, as well as smooth transition from unconstrained
210 to constrained (and vice versa) robot motion are used for controlling the robot arm job-task. The load
211 cell signal processing and the human-machine interface were implemented in MatLab (R2016b,
212 MathWorks, Natick, MA, USA).

213 The load cell mounts a spring-like shaped 3D-printed indenter made of PLA. The particular
214 spring-like shape of the indenter allows to bend its terminal part in all directions, thus reducing
215 overall stiffness of the robot arm, to avoid excessive contact forces and breakage. On the terminal part
216 of the 3D printed indenter a polymeric soft fingertip is mounted, which is used to press the selected
217 pushbuttons placed on a test bench in front of the robotic arm. This dedicated touchpad was designed
218 and developed to evaluate the performance of the remote-controlled robotic platform. It consists of 6
219 push-button tasters, equipped with integrated LED based light indicators, together with a
220 microcontroller-based control system for switching the integrated LED indicators, as well as the
221 electrical state of the push-button tasters. The lighting of LED indicators follows randomly generated

222 sequences of switching order, and the light is switched off when the fingertip properly presses the
 223 push-button.

224 The three subsystems described above are interconnected in the experimental environment as
 225 represented in Figure 3.



226

227 **Figure 3. Scenario of the remote robot control experiment.** (A) Haptic glove for vibrotactile feedback
 228 on the user hand, equipped with two vibrotactile piezoelectric actuators; (B) Marker-less hand
 229 tracking device (Leap Motion controller) used to remotely intuitively control the robot movements;
 230 (C) PC with dedicated electronics for the Leap Motion data acquisition and elaboration, to control
 231 the robot and to implement the neuronal spiking model for the generation of the vibrotactile
 232 feedback; (D) PC with dedicated electronics for the robotic arm control and activation of the LEDs
 233 on the push-button taster. The PC receives data from the hand tracking device; (E) Robotic arm; (F)
 234 Robotic arm end effector on which a polymeric finger is installed by means of a 3D printed compliant
 235 support, and a load cell for force measurements; (G) Touch-pad made of six push-buttons equipped
 236 with LED to be pushed during the experiment following a random sequence. The numbers in figure
 237 are representative of the data flow across the components of the experimental scenario.

238 2.4 Data analysis methods and statistical tests

239 Data analysis was performed using the Statistics Toolbox in MatLab (R2016b, MathWorks,
 240 Natick, MA, USA). The median and the interquartile range of different experimental parameters were
 241 calculated and represented with boxplots, in order to evaluate differences between groups in the two
 242 experimental conditions ('no feedback'/'feedback'). This analysis was performed on the number of
 243 pressed buttons in each trial, to investigate the participants performance for each condition.
 244 Significant differences between groups were analyzed with the Kruskal-Wallis test.

245

246

247

248 2.5 Participants

249 Fourteen healthy subjects (1 female and 13 males) aged between 23 and 34, mean age 26.5,
250 participated in the experiments. Haptic stimulation was performed on the subject's right hand, that
251 for all participants was the dominant. None of them self-reported to have previously performed any
252 activity presumably compromising finger tactile sensitivity, nor had previous contact with our
253 system, nor had received any previous training.

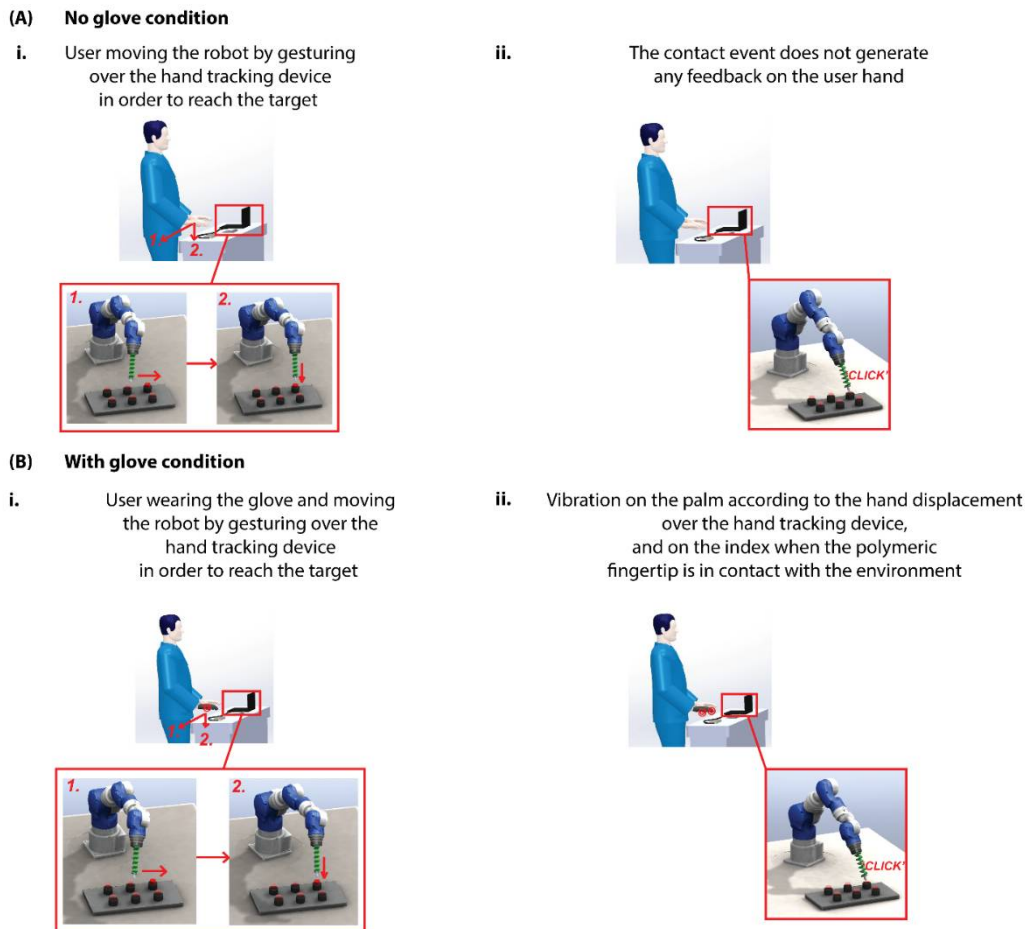
254 2.6 Experimental protocol: remote robot control with tactile telepresence

255 The subject is introduced in the experiment room, where he/she is briefly informed about the
256 experiment aim and the protocols. Experimenters are always present in the room but do not interfere
257 with the volunteers. The aim of the experiment is the quantitative evaluation of the performance (the
258 number of pressed buttons in each experimental session) of the gesture-based robot control system
259 in two different configurations (Figure 4): 1) without tactile feedback; 2) with tactile feedback. To
260 satisfy this purpose, the subject is asked to remotely guide the robot over the dedicated touch-pad
261 and to press the button corresponding to a lighted LED by means of the robot fingertip, being as
262 quick as possible in performing this operation. Subjects are divided in two groups, each one
263 performing the experimental task as first in one of the two conditions (Figure 4) to evaluate whether
264 the introduction of the haptic feedback has an impact on the participant performance. Each
265 experiment consists of 5 sessions. Each session is 2 minutes long and involves the remote control of
266 the robotic arm to press the lighted LEDs in the presented randomized sequence. Before starting the
267 experiment in each condition, participants are provided with a self-training session of about 2
268 minutes to familiarize with the system and with the task. The total duration of the experiment is
269 around 15 minutes, 20 minutes including training. Participants are allowed to rest around 1 minute
270 between each repetition, or even more if they need in order to avoid distress.

271 The task starts when the first LED lightens. The subject moves his/her hand over the hand
272 tracking device to control the robot arm movements. Once the target LED is reached, the subject
273 lowers the hand towards the hand tracking device and the robotic fingertip presses the lighted
274 button. If the pressure operation is applied properly and the button completely pressed, the LED is
275 turned off; when the pressure force is released, a new LED indicator of a new, or even the same, push-
276 button taster is turned on. This action is repeated until the time limit of 2 minutes. The microcontroller
277 which controls the LED indicators simultaneously measures the time required by the operator to
278 reach the position of the button, together with the contact force to switch it off (see Figure 4).

279 The computer simultaneously acquires other relevant data from the robot open-control system:
280 1) presence of the hand over the hand tracking device, 2) Cartesian coordinates of the robot TCP (Tool
281 Center Point) set to coincide with the robot fingertip, 3) coordinates and timestamps of the TCP
282 contact force generated by the robot during the button pressing sequence (in fact, constrained robot
283 motion), 4) indexes of which button is lighted and of which button is pressed (if any), 5) gesture-
284 based commands generated by the robot operator, 6) timestamps of the spikes generated by the
285 neuromorphic algorithm which activity is proportional to the force measured by the load cell, for the
286 index transducer, and to the hand displacement, for the palm transducer. The time elapsed between
287 the LED lighting and the pushing of the button which switches it off is instead calculated off-line.

288 Based on this comprehensive information content (time series), it is possible to evaluate
289 quantitative statistical measures of the human operator behavior.



290

291

292

293

294

295

296

297

298

299

300

301

Figure 4. Steps of the experimental protocol for the remote-control experiment with tactile telepresence in the two experimental conditions. (A) No-glove condition: i. The user moves the hand over the hand tracking device in order to move the robotic arm laterally (1.), and down (2.) to reach the lighted button; ii. Once the targeted push-button is reached, the user taps over the hand tracking device to lower the robotic arm and pushes the button down; **(B) Glove condition:** i. The user wearing the vibro-tactile glove moves the hand over the hand tracking device in order to move the robotic arm laterally (1.), and down (2.) to reach the lighted button, receiving vibrotactile feedback on the palm; ii. Once the targeted push-button is reached, the user taps over the hand tracking device to lower the robotic arm and pushes the button down, receiving vibrotactile feedback on the index fingertip when the polymeric fingertip on the robot end-effector is in contact with the environment, and on the palm according to the movement of the hand over the hand tracking device.

302

3. Results

303

The proposed architecture for the bidirectional remote control of the robotic arm is effective and intuitive, and the introduction of neuromorphic vibrotactile feedback can improve the user awareness during the execution of a task, with measurable effects on performance.

304

305

306

307

308

309

310

311

312

313

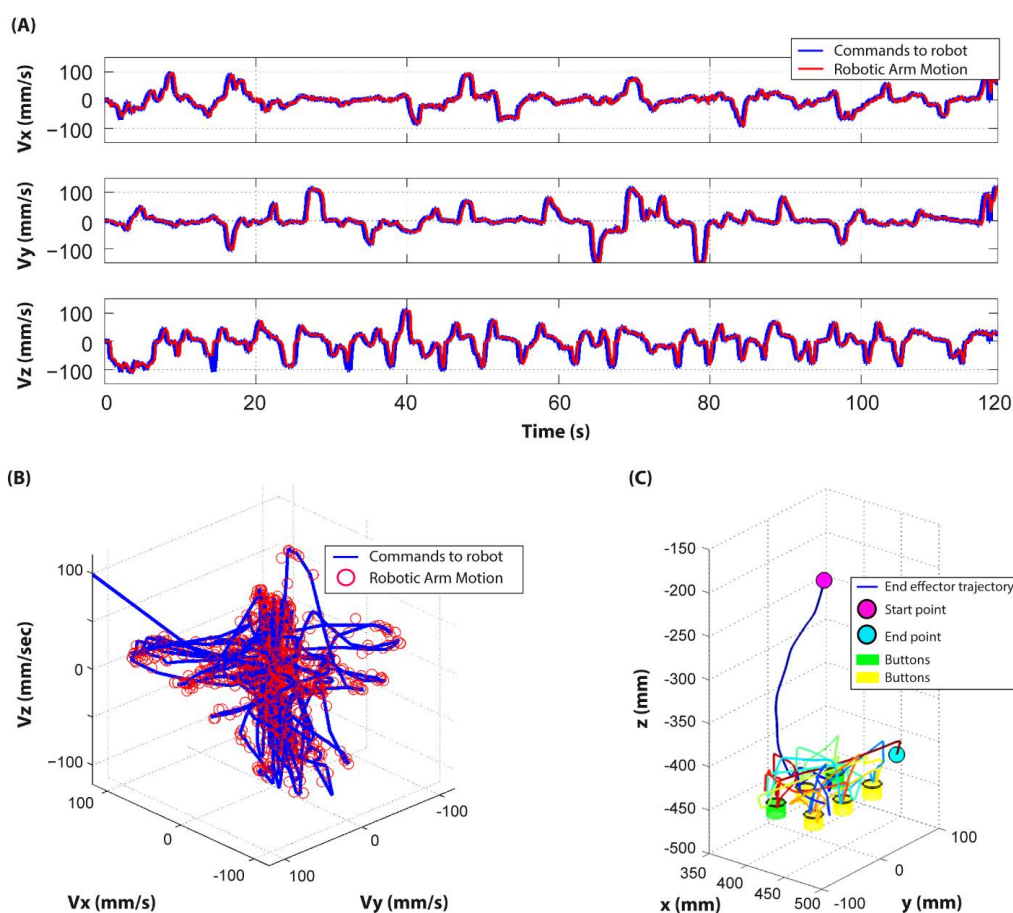
314

The purpose of this experiment is to evaluate whether the hand tracking recognition input, coupled with the neuromorphic vibrotactile feedback, provides an effective channel for bidirectional human-machine interaction.

315 3.1 Robot trajectories and velocities versus commanded movements via the gesture-based control

316 We first evaluated the capability of the hand tracking device in the detection of the hands
 317 movements in order to control the robotic arm. We used an intuitive approach in which hand posture
 318 and motion were transformed into specific commands to be sent to the robot (see Figure 2 for the
 319 correspondence between the hand commands and the robot movements).

320 The hand position and velocity profiles were acquired during the execution of the task in both
 321 the experimental conditions. These profiles were then compared with the trajectory of the robotic arm
 322 velocity during the execution of the task. The velocity profile commanded via the hand tracking
 323 device and the corresponding profile of the robotic arm velocity are overlapped in Figure 5 (A).
 324 Results showed how the robotic arm is capable to follow the movements of the hand over the hand
 325 tracking device. This confirms that the implemented algorithm for the robot control has a suitable
 326 dynamics so to enable the robotic arm to follow the hand trajectory and velocity in a reliable manner.
 327 The reliability of the gesture-based control is also detectable from the analysis of the commanded
 328 velocity profile versus the corresponding robot velocity (see Figure 5 (B)) within the three-
 329 dimensional experimental workspace (see Figure 5 (C)).



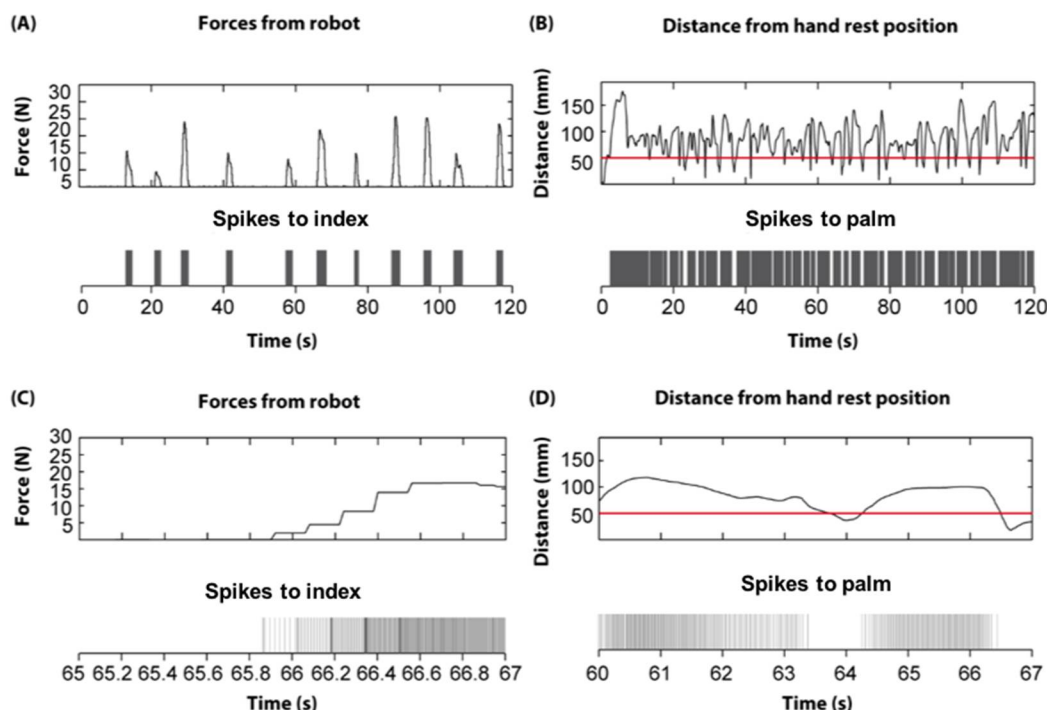
330

331 **Figure 5. Speed of robotic arm along the three axes vs. manual commands from the hand tracking**
 332 **device.** (A) Behaviour of the velocity of the hand commands sent to the robot via the hand tracking
 333 device (red line) vs. real motion of the robotic arm (blue line); (B) Spatial representation of the
 334 commanded motion velocity coming from the hand tracking device (blue line) and of the robotic arm
 335 velocity (red dots) in the 3D space; (C) Trajectory of the robot end-effector while pressing the buttons
 336 during the experimental session, with starting and ending points.

337 3.2 Neuromorphic haptic feedback during the experimental task

338 Figure 6 reports an example of spiking activity released by the transducers of the haptic glove
 339 during the execution of a remote-control task. The spiking activity on the index fingertip is

340 representative of the forces exerted by the robot end-effector, and measured by the load cell
 341 (exteroceptive feedback). The generation of the spikes is mediated by the Izhikevich artificial neuron
 342 spiking model (see Section 2.2) and is then conveyed to the transducer placed on the index fingertip.
 343 As the force value increases, the rate of spikes delivered to the index fingertip increases, while the
 344 absence of spikes means that no contact events are detected (Figure 6 (A, C)). The spiking activity on
 345 the hand palm is instead representative of the hand distance with respect to the rest position over the
 346 hand tracking device (proprioceptive feedback), corresponding to the commanded robot velocity. A
 347 higher distance from the rest position generates a more intense spiking activity, while the absence of
 348 the hand over the sensor (hand not detected/hand out of the workspace) corresponds to the absence
 349 of vibration (see Figure 6 (B, D)).



350

351 **Figure 6. Figure of spike trains for one trial.** (A) (upper panel) Forces exerted from the robot when
 352 indenting the buttons (upper panel); Spike trains transduced to the glove index, which activity is
 353 proportional to the amount of force measured by the load cell mounted on the robot end-effector
 354 (lower panel); (B) Distance from the hand rest position (represented as a red line) acquired by the
 355 hand tracking device while the user hand is moving to control the robotic arm (upper panel); (B)
 356 Spike trains transduced to the glove palm, which activity is proportional to the hand distance respect
 357 to the hand rest position (lower panel); (C) Forces exerted from the robot during one single button
 358 pressure (upper panel); (C) Spike trains transduced to the glove index during one single button
 359 pressure (lower panel); (D) Distance from the hand rest position (represented as a red line) acquired
 360 by the hand tracking device during one single button pressure (upper panel); (D) Spike trains
 361 transduced to the glove palm during the operations executed for commanding one single button
 362 pressure, which activity is proportional to the hand velocity respect to the hand rest position (lower
 363 panel).

364 **3.3 Evaluation of the participants performance in completing the task via the gesture-controlled robot, with or**
 365 **without tactile feedback**

366 To evaluate whether the provision of tactile feedback has an effect on the participants
 367 performance during the execution of the task, we compared the results from the group performing
 368 the experiment in the 'no feedback' condition with those from the group performing the 'feedback'
 369 condition (Video S1). **Table 1** reports the median number of completed tasks, across all participants,
 370 for each experimental session in the two conditions. The median values and interquartile ranges for
 371 the two experimental conditions are reported in Figure 7, relative to all the experimental trials for all

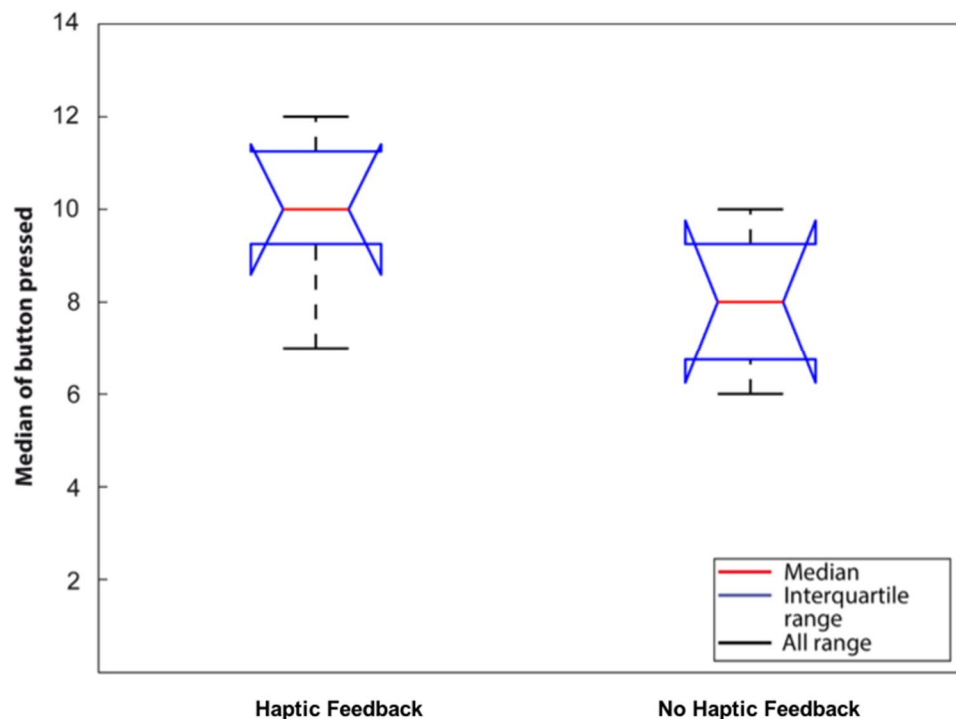
372 participants. The median values for the 'feedback' condition are systematically higher than those
 373 relative to the 'no feedback' condition. This can be indicative of an effect on the improvement of user
 374 learning performance and confidence with the task when tactile feedback is provided.

375
 376
 377

Table 1. Number of button hits. Median values of the number of button hits for the two experimental conditions.

Trial No.	With glove (median)	No glove (median)
1	7	6
2	11	9
3	10	7
4	10	8
5	12	10
<i>All trials</i>	10	8

378



379

380 **Figure 7. Boxplot of the number of buttons pressed in the two experimented conditions.** Median
 381 and interquartile range of the number of buttons pressed by all participants in the two experimental
 382 conditions. The first box represents the trials performed by the 'feedback' condition group, while the
 383 second box represents the trials performed by the 'no feedback' condition group.

384 4. Discussion and conclusions

385 We described an intuitive gesture-based system for the remote control of a robotic arm with
 386 tactile telepresence, which allows the users to perform a pick-and-place-like industrial task. Tactile

387 feedback was delivered via a textile glove equipped with customized piezoelectric actuators.
388 Vibrotactile information was generated according to neuronal spiking models and delivered directly
389 on the hand palm, with a rate proportional to the hand displacement over a hand-tracking device,
390 and on the fingertip of the index, with a rate proportional to the contact forces exerted by the robot
391 end-effector.

392 Our system has been tested with untrained volunteers, both in the cases where tactile feedback
393 was or was not provided, on an experimental pipeline aimed at emulating activities that can be
394 typically encountered in an industrial context as well as in a whelm of robot remote control
395 applications.

396 The analysis of experimental data shows that the commands acquired via the hand tracking
397 device are always coherent with the real robot motion executed. Furthermore, all the participants
398 demonstrated to easily interact with the experimental set-up, and none of them needed more than
399 one training session to master it. Participants performance in the execution of the task resulted overall
400 good and increased when tactile feedback was provided. Furthermore, participants reported an
401 increased awareness of the robot movements and exerted forces when tactile feedback was provided.

402 The marker-less technology of the hand tracking device enabled participants to wear the glove
403 and receive tactile feedback during the experimental task without affecting the tracking performance.
404 Furthermore, since the hand tracking is independent from the variation of anthropometry of the
405 human hand, it can allow a very large applicability.

406 With our work, we contributed to demonstrate vibrotactile feedback for human-robot co-
407 working activities, in particular when performing telepresence tasks. Haptic devices can be of
408 paramount importance when used in environments where the interaction with automated machinery
409 can be dangerous for operators. Haptic feedback can in fact be used to deliver information about the
410 occurrence of critical events and thus improve workers safety in collaborative robotic tasks. Tactile
411 technologies such as force sensors installed on the robotic end-effectors can acquire information about
412 contact events and exerted forces, enabling a remote user to easily perform precise manipulations
413 and detect slippages. This research will be complemented with future experiments simulating
414 different and more complex activities such as precise manipulation tasks of small objects.

415 **Supplementary Materials:** Video S1: video of the experimental protocol showing the gesture-based robot control
416 task being performed with and without haptic feedback.

417 **Author Contributions:** F.S. designed the experimental protocol, developed the haptic glove and integrated the
418 experimental setup, performed the principal experimental protocol, analyzed data, discussed the results and
419 wrote the paper; G.A.F. designed the experimental protocol, integrated the experimental setup, performed the
420 principal experimental protocol, analyzed data, discussed the results and wrote the paper; N.L. co-designed the
421 experimental protocol, developed and programmed the robotic arm system, analyzed data, discussed the results
422 and contributed to writing the paper; I.D. co-designed the experimental protocol, developed and programmed
423 the robotic arm system, analyzed data, discussed the results and contributed to writing the paper; B.B.
424 contributed to designing the experimental protocol, contributed to discussion of results and revised the paper;
425 M.M. designed and fabricated parts of the experimental setup and revised the paper; T.B.P. contributed to
426 analyzing data and revised the paper; L.R. contributed to discussing the results and revised the paper; P.P.
427 provided background in computer engineering, contributed to discussing the results and revised the paper; T.T.
428 provided engineering background in production engineering, contributed to discussing the results and revised
429 the paper, M.C.C. provided background in bioengineering, co-supervised the development of the haptic glove,
430 contributed to discussing the results and revised the paper; P.B.P. co-designed and co-supervised the study, co-
431 supervised the development of the whole experimental apparatus and contributed to its development, co-
432 designed the experimental protocol, contributed to data analysis, discussed the results and contributed to
433 writing the paper; C.M.O. designed and supervised the study, supervised the development of the whole
434 experimental apparatus and contributed to its development, ideated the neuromorphic haptic feedback strategy,
435 designed the experimental protocol, contributed to data analysis, discussed the results and wrote the paper.

436 **Funding:** This research was funded in part by the Italian Ministry of Education, Universities and Research within
437 the "Smart Cities and Social Innovation Under 30" program through the PARLOMA Project (SIN_00132) and by
438 the Italian Ministry of Foreign Affairs and International Cooperation via the Italy-Serbia bilateral project
439 Human-Robot Co-Working as a Key Enabling Technology for the Factories of Future (project ID: PGR00758 /

440 2017). This project received seed funding from the Dubai Future Foundation through Guaana.com open research
441 platform.

442 **Conflicts of Interest:** The authors declare no conflict of interest. The funders had no role in the design of the
443 study; in the collection, analyses, or interpretation of data; in the writing of the manuscript, or in the decision to
444 publish the results.

445 References

- 446 1. Lipton, J.I.; Fay, A.J.; Rus, D. Baxter's homunculus: Virtual reality spaces for teleoperation in
447 manufacturing. *IEEE Robotics and Automation Letters* **2018**, *3*, 179-186.
- 448 2. Sheridan, T.B. Human-robot interaction: Status and challenges. *Human factors* **2016**, *58*, 525-532.
- 449 3. Sibert, J.; Cooper, J.; Covington, C.; Stefanovski, A.; Thompson, D.; Lindeman, R.W. In *Vibrotactile feedback for*
450 *enhanced control of urban search and rescue robots*, Proceedings of the IEEE International Workshop on Safety,
451 Security and Rescue Robotics, 2006.
- 452 4. Iborra, A.; Pastor, J.A.; Alvarez, B.; Fernandez, C.; Merono, J.M.F. Robots in radioactive environments. *IEEE*
453 *Robotics & Automation Magazine* **2003**, *10*, 12-22.
- 454 5. Lester, D.F.; Hodges, K.V.; Anderson, R.C. Exploration telepresence: A strategy for optimizing scientific
455 research at remote space destinations. *Sci. Robot.* **2017**, *2*, ean4383.
- 456 6. Eltaib, M.; Hewit, J. Tactile sensing technology for minimal access surgery—a review. *Mechatronics* **2003**,
457 *13*, 1163-1177.
- 458 7. Tavakoli, M.; Patel, R.V.; Moallem, M. In *A force reflective master-slave system for minimally invasive surgery*,
459 *Intelligent Robots and Systems, 2003. (IROS 2003)*. Proceedings. 2003 IEEE/RSJ International Conference on,
460 2003; IEEE: pp 3077-3082.
- 461 8. Hokayem, P.F.; Spong, M.W. Bilateral teleoperation: An historical survey. *Automatica* **2006**, *42*, 2035-2057.
- 462 9. Passenberg, C.; Peer, A.; Buss, M. A survey of environment-, operator-, and task-adapted controllers for
463 teleoperation systems. *Mechatronics* **2010**, *20*, 787-801.
- 464 10. Wachs, J.P.; Kölsch, M.; Stern, H.; Edan, Y. Vision-based hand-gesture applications. *Communications of the*
465 *ACM* **2011**, *54*, 60-71.
- 466 11. Russo, L.O.; Farulla, G.A.; Pianu, D.; Salgarella, A.R.; Controzzi, M.; Cipriani, C.; Oddo, C.M.; Geraci, C.;
467 Rosa, S.; Indaco, M. Parloma-a novel human-robot interaction system for deaf-blind remote
468 communication. *International Journal of Advanced Robotic Systems* **2015**, *12*.
- 469 12. Airò Farulla, G.; Pianu, D.; Cempini, M.; Cortese, M.; Russo, L.O.; Indaco, M.; Nerino, R.; Chimienti, A.;
470 Oddo, C.M.; Vitiello, N. Vision-based pose estimation for robot-mediated hand telerehabilitation. *Sensors*
471 **2016**, *16*, 208.
- 472 13. Malis, E. Survey of vision-based robot control. *ENSIETA European Naval Ship Design Short Course, Brest,*
473 *France* **2002**.
- 474 14. Thompson, J.L. Redesigning the human-robot interface: Intuitive teleoperation of anthropomorphic robots.
475 2014.
- 476 15. Motion, L. Leap motion controller. www.leapmotion.com (October 10),
- 477 16. Guerrero-Rincon, C.; Uribe-Quevedo, A.; Leon-Rodriguez, H.; Park, J.-O. In *Hand-based tracking*
478 *animatronics interaction*, Robotics (ISR), 2013 44th International Symposium on, 2013; IEEE: pp 1-3.
- 479 17. Kruusamäe, K.; Pryor, M. In *High-precision telerobot with human-centered variable perspective and scalable*
480 *gestural interface*, Human System Interactions (HSI), 2016 9th International Conference on, 2016; IEEE: pp
481 190-196.
- 482 18. Weichert, F.; Bachmann, D.; Rudak, B.; Fisseler, D. Analysis of the accuracy and robustness of the leap
483 motion controller. *Sensors* **2013**, *13*, 6380-6393.
- 484 19. Marin, G.; Dominio, F.; Zanuttigh, P. In *Hand gesture recognition with leap motion and kinect devices*, 2014 IEEE
485 International Conference on Image Processing (ICIP), 2014; IEEE: pp 1565-1569.
- 486 20. Choi, S.; Kuchenbecker, K.J. Vibrotactile display: Perception, technology, and applications. *Proceedings of*
487 *the IEEE* **2013**, *101*, 2093-2104.
- 488 21. Sziebig, G.; Solvang, B.; Kiss, C.; Korondi, P. In *Vibro-tactile feedback for vr systems*, Human System
489 Interactions, 2009. HSI'09. 2nd Conference on, 2009; IEEE: pp 406-410.
- 490 22. Alahakone, A.U.; Senanayake, S.; Arosha, M. In *Vibrotactile feedback systems: Current trends in rehabilitation,*
491 *sports and information display*, Advanced Intelligent Mechatronics, 2009. AIM 2009. IEEE/ASME
492 International Conference on, 2009; IEEE: pp 1148-1153.

- 493 23. Galambos, P. Vibrotactile feedback for haptics and telemanipulation: Survey, concept and experiment. *Acta*
494 *Polytechnica Hungarica* **2012**, *9*, 41-65.
- 495 24. Jones, L.A.; Lederman, S.J. Tactile sensing. In *Human hand function*, Jones, L.A.; Lederman, S.J., Eds. Oxford
496 University Press: 2006; p 62.
- 497 25. Kandel, E.R.; Schwartz, J.H.; Jessell, T.M. *Principles of neural science* 4th ed.; McGraw-Hill Medical: 2000.
- 498 26. Brewster, S.; Brown, L.M. In *Tactons: Structured tactile messages for non-visual information display*, Proceedings
499 of the fifth conference on Australasian user interface-Volume 28, 2004; Australian Computer Society, Inc.:
500 pp 15-23.
- 501 27. Gunther, E.; O'Modhrain, S. Cutaneous grooves: Composing for the sense of touch. *Journal of New Music*
502 *Research* **2003**, *32*, 369-381.
- 503 28. Vallbo, Å.B.; Johansson, R.S. Properties of cutaneous mechanoreceptors in the human hand related to touch
504 sensation. *Hum Neurobiol* **1984**, *3*, 3-14.
- 505 29. Verrillo, R.T. Psychophysics of vibrotactile stimulation. *The Journal of the Acoustical Society of America* **1985**,
506 *77*, 225-232.
- 507 30. Liu, Y.; Yu, Y.; Yang, J.; Inai, Y.; Wu, J. In *Ability to recognize and identify the location of vibration stimulation*
508 *on the fingers*, Mechatronics and Automation (ICMA), 2014 IEEE International Conference on, 2014; IEEE:
509 pp 1601-1606.
- 510 31. Robles-De-La-Torre, G. The importance of the sense of touch in virtual and real environments. *Ieee*
511 *Multimedia* **2006**, *13*, 24-30.
- 512 32. Tegin, J.; Wikander, J. Tactile sensing in intelligent robotic manipulation-a review. *Industrial Robot: An*
513 *International Journal* **2005**, *32*, 64-70.
- 514 33. Sorgini, F.; Mazzoni, A.; Massari, L.; Caliò, R.; Galassi, C.; Kukreja, S.; Sinibaldi, E.; Carrozza, M.; Oddo, C.
515 Encapsulation of piezoelectric transducers for sensory augmentation and substitution with wearable haptic
516 devices. *Micromachines* **2017**, *8*, 270.
- 517 34. Sorgini F, G.R., Huebotter JF., Caliò R, Galassi C, Oddo CM., Kukreja SL. Design and preliminary
518 evaluation of haptic devices for upper limb stimulation and integration within a virtual reality cave. *6th*
519 *IEEE RAS/EMBS International Conference on Biomedical Robotics and Biomechatronics. IEEE, 2016.* **2016**, *6*.
- 520 35. Izhikevich, E.M. Simple model of spiking neurons. *IEEE Transactions on neural networks* **2003**, *14*, 1569-1572.
- 521 36. Sorgini, F.; Massari, L.; D'Abbraccio, J.; Palermo, E.; Menciassi, A.; Petrovic, P.B.; Mazzoni, A.; Carrozza,
522 M.C.; Newell, F.N.; Oddo, C.M. Neuromorphic vibrotactile stimulation of fingertips for encoding object
523 stiffness in telepresence sensory substitution and augmentation applications. *Sensors* **2018**, *18*, 261.
- 524 37. Ott, C. Cartesian impedance control: The rigid body case. In *Cartesian impedance control of redundant and*
525 *flexible-joint robots*, Springer: 2008; pp 29-44.
- 526 38. Ott, C.; Albu-Schaffer, A.; Kugi, A.; Stamigioli, S.; Hirzinger, G. In *A passivity based cartesian impedance*
527 *controller for flexible joint robots-part i: Torque feedback and gravity compensation*, Robotics and Automation,
528 2004. Proceedings. ICRA'04. 2004 IEEE International Conference on, 2004; IEEE: pp 2659-2665.
529